Discovery of Carbon-11 Labeled Sulfonamide Derivative: A PET Tracer for Imaging Brain NLRP3 Inflammasome

Yulong Xu[a], **Yiming Xu**[b], **Hallie Blevins**[b], **Yu Lan**[a], **Yan Liu**[a], **Gengyang Yuan**[d], **Robin M. Striar**[a], **Julia S. Zagaroli**[a], **Darcy R. Tocci**[a], **Amelia G. Langan**[a], **Can Zhang**[c], **Shijun Zhang**[b], **Changning Wang**[a,*]

[a]Athinoula A. Martinos Center for Biomedical Imaging, Department of Radiology, Massachusetts General Hospital, Harvard Medical School, Charlestown, Massachusetts 02129, United States

[b]Department of Medicinal Chemistry, Virginia Commonwealth University, Richmond, Virginia 23298, United States

[c]Genetics and Aging Research Unit, McCance Center for Brain Health, MassGeneral Institute for Neurodegenerative Disease, Department of Neurology, Massachusetts General Hospital, Harvard Medical School, Charlestown, Massachusetts 02129, United States

[d]Gordon Center for Medical Imaging, Massachusetts General Hospital, Harvard Medical School, Charlestown, Massachusetts 02129, United States

Abstract

We report herein the discovery of a positron emission tomography (PET) tracer for the (NOD)-like receptor protein 3 (NLRP3). Our recent medicinal chemistry campaign on developing sulfonamide-based NLRP3 inhibitors led to an analog, **1**, with a methoxy substituent amenable to labeling with carbon-11. PET/CT imaging studies indicated that [^{11}C]**1** exhibited rapid blood-brain barrier (BBB) penetration and moderate brain uptake, as well as blockable uptake in the brain. [^{11}C]**1**, thus suggesting the potential to serve as a useful tool for imaging NLRP3 inflammasome in living brains.

Graphical Abstract
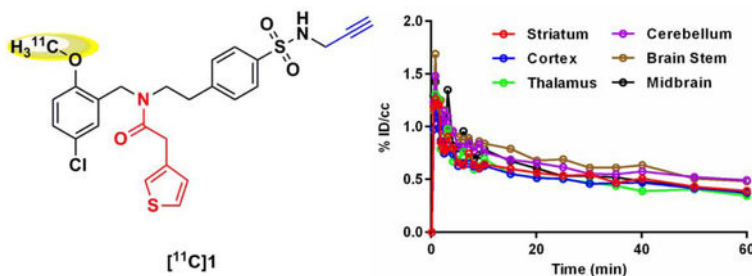
*Corresponding author. cwang15@mgh.harvard.edu (C. Wang).

$[^{11}C]1$

Keywords

NLRP3; Positron emission tomography (PET); Sulfonamide derivative; Blood-brain barrier (BBB) penetration; Blockable uptake

Inflammasomes are intracellular and multimeric protein complexes that mediate the innate immune response and the release of pro-inflammatory cytokines, i.e., interleukin (IL)-1β and IL-18.[1] Inflammasomes that have been characterized include the nucleotide oligomerization domain (NOD)-like receptor (NLR) family, the absent in melanoma 2 (AIM2), and retinoic acid-inducible gene I (RIG-I)-like receptor (RLR).[2] Among these, the NLRP3 inflammasome has been extensively studied, and its essential roles in detecting a plethora of danger signals such as danger associated molecular patterns (DAMPs) and pathogen associated molecular patterns (PAMPs) have been well documented.[3] Aberrant activation of the NLRP3 inflammasome has been observed in the pathogenesis of numerous human disorders, including auto-inflammatory and auto-immune diseases, diabetes, and neurodegenerative diseases.[4–7] Therefore, inhibition of the NLRP3 inflammasome has attracted great interests as a promising strategy to achieve disease interventions.

To better understand the NLRP3 biology and assist drug discovery that targets the NLRP3 inflammasome, a suitable single photon emission computed tomography (SPECT) or positron emission tomography (PET) tracer will be valuable. Such tracers will allow for visualization of the NLRP3 inflammasome in living organs under normal and disease conditions with minimal perturbation of the biological state, and this is particularly essential for central nervous system (CNS) drug discovery. PET is a well-established noninvasive imaging modality, providing valuable information on target expression, occupancy and biodistribution.[8–10] A number of structurally diverse inhibitors targeting this inflammasome have recently been reported, including benzenesulfonamide-based derivatives, sulfonylurea analogs, boron derivatives, acrylate derivatives, and acrylamide derivatives, among others (Fig. 1).[11–18] To the best of our knowledge, only a sulfonylurea based PET tracer, [^{11}C]MCC950, has been developed and characterized in healthy mouse, rat and rhesus monkey.[19] However, PET imaging studies of this tracer revealed its poor brain uptake and rapid washout.[19] Therefore, PET tracers of the NLRP3 inflammasome with desirable properties to enable the preclinical and clinical characterizations of NLRP3 inflammasome are urgently needed. As our continuing interests in developing CNS PET tracers, herein, we are reporting the characterization of a carbon-11 labeled sulfonamide-based NLRP3 inhibitor as a novel PET tracer for imaging brain NLRP3 inflammasome.[20–22]

The initial lead compound, **JC124**, was identified as a selective inhibitor that directly targets the NLRP3 inflammasome complex with an IC_{50} of 3.25 ± 1.34 μM by our group (Fig. 2).[12] To improve the inhibitory potency and pharmacokinetic properties, medicinal chemistry campaign led to the identification of **YQ128** with significantly improved inhibitory potency ($IC_{50} = 0.30 \pm 0.01$ μM) and retained selectivity to the NLRP3 inflammasome.[23] Further studies also demonstrated its blood-brain barrier (BBB) penetration in mice. Despite the favorable biological properties, a reliable route for radiolabeling **YQ128** was not feasible. Thus, our efforts were focused on sulfonamide **1**, an analog of **YQ128** with comparable potency ($IC_{50} = 0.90 \pm 0.06$ μM, Clog $P = 4.548$) to develop a PET tracer by taking advantage of the *O*-methyl substituent that is amenable to labeling with carbon-11.

The chemical synthesis of sulfonamide **1** and **[^{11}C]1** is outlined in Scheme 1. Briefly, reaction of sulfonyl chloride **2** with propargylamine **3** yielded compound **4** in 75% yield. Compound **4** was then deprotected with methylhydrazine followed by reduction amination with aldehyde **7** to give compound **8**. Coupling reaction of **8** with 3-thiopheneacetic acid to afford sulfonamide **1** in 57% yield. TBS-protected aldehyde **6** was reacted with amine **5** and followed by the removal of TBS protecting group in the presence of TBAF and coupling reaction with 3-thiopheneacetic acid to give precursor **10**. Radiosynthesis of **[^{11}C]1** was successfully achieved by the methylation of precursor **10** with [^{11}C]CH_3I. **[^{11}C]1** was afforded with a radiochemical yield of $49 \pm 10\%$ (n = 3, decay corrected). Total synthesis time from the end of cyclotron bombardment was 38 ± 3 min. The resultant **[^{11}C]1** was reformulated via solid-phase exchange (SPE) C-18 cartridge and reconstituted in sterile saline containing <10% (v/v) ethanol. Quality control testing confirmed radiochemical purities >99%, molar radioactivity = 418 GBq/μmol at time of injection.

[a] Reagents and conditions: (i): Trimethylamine, CH_2Cl_2, rt. (ii): NH_2NH_2, EtOH, 60 °C. (iii): Iodomethane, K_2CO_3, DMF, rt. (iv): 1. amine **5**, trimethylamine, MeOH, rt; 2. Acetic acid, $NaCNBH_3$, MeOH, rt. (v): 3-Thiopheneacetic acid, EDCI (1-(3-dimethylaminopropyl)-3-ethylcarbodiimide hydrochloride), HOBt (1-hydroxybenzotriazole), trimethylamine, CH_2Cl_2, rt. (vi): TBSCl, imidazole, CH_2Cl_2, rt. (vii): 1. amine **5**, trimethylamine, MeOH, rt; 2. Acetic acid, $NaCNBH_3$, MeOH, rt; 3. 1M TBAF, THF, rt; 4. 3-Thiopheneacetic acid, EDCI, HOBt, trimethylamine, CH_2Cl_2, rt. (viii): [^{11}C]CH_3I, K_2CO_3, DMF, 80 °C.

Next, **[^{11}C]1** was characterized by PET/CT scanning in isoflurane anesthetized C57BL/6 mice (24–26 g, male) after a single intravenously administration (~7.4 MBq). The data were expressed as the percentage of injected dose per cubic centimetre (% ID/cc) and plotted for the 60 min scan window. As shown in Fig. 3, radioactivity in organs of interest was quantified to measure accumulation of **[^{11}C]1** and to determine potential metabolic pathways of **[^{11}C]1**. Significant and quick initial uptakes in blood and liver (10.15% ID/cc and 22.60% ID/cc at 2 min post injection, respectively) were observed, followed by fast clearance (1.92% ID/cc and 8.41% ID/cc at 60 min post injection, respectively). **[^{11}C]1** also showed significant initial uptake in intestine (10.58% ID/cc at 2 min post injection), then increased rapidly (43.43% ID/cc at 60 min post injection). This may suggest that **[^{11}C]1** is mainly excreted through feces. The lung uptake peaked at 2 min (8.73% ID/cc) and washed

out rapidly (1.76% ID/cc at 60 min post injection). Compared with other organs, the uptake of [^{11}C]1 in heart, kidney and muscle was low and decreased slowly over time.

Next, we investigated the brain uptake of [^{11}C]1 as the sulfonamide based NLRP3 inhibitors were designed as potential CNS agents for Alzheimer's disease. As shown in Fig. 4, the baseline studies (n = 2) demonstrated that [^{11}C]1 rapidly crossed the BBB and accumulated in the brain regions homogeneously. [^{11}C]1 exhibited moderate brain uptake with a maximum signal of ~1.7 % ID/cc at 1 min post injection. The signal declined rapidly to ~0.9 % ID/cc at 5 min post injection. Self-blocking studies (n = 2) with sulfonamide 1 revealed that the specific signal ratio (total signal ratio/nonspecific signal ratio) was ~1.4:1 after 15 min post injection, close to the criteria of a desirable CNS PET tracer (specific signal ratio = ~1.5:1).[24] Notably, the accumulation of [^{11}C]1 in thyroid gland was blocked by sulfonamide 1, indicating specific binding of [^{11}C]1 to thyroid gland NLRP3 (26% specific binding at 60 min, listed in Support Information, Fig. S3), which suggested that [^{11}C]1 could be a suitable PET tracer for imaging tumors in the thyroid gland. However, compared to the desirable properties of a successful CNS PET tracer, the brain uptake of [^{11}C]1 still needs to be optimized. [^{11}C]1, therefore, can serve as a lead compound for the further structural exploration and optimization studies. Collectively, the results strongly encourage further studies of [^{11}C]1 in preclinical models of neurodegenerative disorders with aberrant activation of NLRP3 and development of optimized PET tracers based on this chemical scaffold.

In conclusion, a novel PET tracer for the NLRP3 inflammasome, [^{11}C]1, was synthesized and characterized through PET/CT imaging studies in C57BL/6 mice. [^{11}C]1 exhibited rapid BBB penetration and moderate brain uptake, as well as blockable uptake in brain. This tracer successfully resulted in visualization of NLRP3 physiological condition in animal brains. Thus, [^{11}C]1 serves as a useful tool with the potential to characterize NLRP3 inflammasome in living brains linked to various NLRP3-related neurological conditions.

Supplementary Material

Refer to Web version on PubMed Central for supplementary material.

Acknowledgments

References

1. Martinon F, Burns K, Tschopp J. The inflammasome: a molecular platform triggering activation of inflammatory caspases and processing of proIL-beta. Mol Cell. 2002;10(2):417–426. [PubMed: 12191486]

2. Schroder K, Tschopp J. The Inflammasomes. Cell. 2010;140(6):821–832. [PubMed: 20303873]

3. Chen G, Shaw MH, Kim YG, Nuñez G. NOD-like receptors: role in innate immunity and inflammatory disease. Annu Rev Pathol. 2009;4:365–398. [PubMed: 18928408]

4. Heneka MT, Kummer MP, Stutz A, et al. NLRP3 is activated in Alzheimer's disease and contributes to pathology in APP/PS1 mice. Nature. 2013;493(7434):674–678. [PubMed: 23254930]

5. Zhou R, Tardivel A, Thorens B, Choi I, Tschopp J. Thioredoxin-interacting protein links oxidative stress to inflammasome activation. Nat Immunol. 2010;11(2):136–140. [PubMed: 20023662]

6. Duewell P, Kono H, Rayner KJ, et al. NLRP3 inflammasomes are required for atherogenesis and activated by cholesterol crystals. Nature. 2010;464(7293):1357–1361. [PubMed: 20428172]

7. Martinon F, Petrilli V, Mayor A, Tardivel A, Tschopp J. Gout-associated uric acid crystals activate the NALP3 inflammasome. Nature. 2006;440(7081):237–241. [PubMed: 16407889]

8. Ametamey SM, Honer M, Schubiger PA. Molecular imaging with PET. Chem Rev. 2008;108:1501–1516. [PubMed: 18426240]

9. Willmann JK, van Bruggen N, Dinkelborg LM, Gambhir SS. Molecular imaging in drug development. Nat Rev Drug Discovery. 2008;7:591–607. [PubMed: 18591980]

10. Miller PW, Long NJ, Vilar R, Gee AD. Synthesis of ^{11}C, ^{18}F, ^{15}O, and ^{13}N radiolabels for positron emission tomography. Angew Chem Int Ed. 2008;47:8998–9033.

11. Lamkanfi M, Mueller JL, Vitari AC, et al. Glyburide inhibits the Cryopyrin/Nalp3 inflammasome. J Cell Biol. 2009;187(1):61–70. [PubMed: 19805629]

12. Fulp J, He L, Toldo S, et al. Structural insights of benzenesulfonamide analogues as NLRP3 inflammasome inhibitors: design, synthesis, and biological characterization. J Med Chem. 2018;61(12):5412–5423. [PubMed: 29877709]

13. Baldwin AG, Rivers-Auty J, Daniels MJD, et al. Boron-based inhibitors of the NLRP3 inflammasome. Cell Chem Biol. 2017;24(11):1321–1335. [PubMed: 28943355]

14. Cocco M, Pellegrini C, Martinez-Banaclocha H, et al. Development of an acrylate derivative targeting the NLRP3 inflammasome for the treatment of inflammatory bowel disease. J Med Chem. 2017;60(9):3656–3671. [PubMed: 28410442]

15. Cocco M, Garella D, Di Stilo A, et al. Electrophilic warhead-based design of compounds preventing NLRP3 inflammasome-dependent pyroptosis. J Med Chem. 2014;57(24):10366–10382. [PubMed: 25418070]

16. Marchetti C, Swartzwelter B, Gamboni F, et al. OLT1177, a β-sulfonyl nitrile compound, safe in humans, inhibits the NLRP3 inflammasome and reverses the metabolic cost of inflammation. Proc Natl Acad Sci USA. 2018;115(7):E1530–E1539. [PubMed: 29378952]

17. Juliana C, Fernandes-Alnemri T, Wu J, et al. Anti-inflammatory compounds parthenolide and Bay 11–7082 are direct inhibitors of the inflammasome. J Biol Chem. 2010;285(13):9792–9802. [PubMed: 20093358]

18. He Y, Varadarajan S, Munoz-Planillo R, Burberry A, Nakamura Y, Nunez G. 3,4-methylenedioxy-beta-nitrostyrene inhibits NLRP3 inflammasome activation by blocking assembly of the inflammasome. J Biol Chem. 2014;289(2):1142–1150. [PubMed: 24265316]

19. Hill JR, Shao X, Massey NL, et al. Synthesis and evaluation of NLRP3-inhibitory sulfonylurea [^{11}C]MCC950 in healthy animals. Bioorg Med Chem Lett. 2020;30(12):127186. [PubMed: 32312583]

20. Chen Z, Wang X, Xu Y, Wang C. Synthesis of ^{11}C-labeled DNA polymerase-• inhibitor 5-methoxyflavone and PET/CT imaging thereof. Nucl Med Biol. 2019;78–79:17–22.

21. Xu Y, Wang Y, Wang H, Wang C. Synthesis and characterization of carbon-11 labeled iloperidone for imaging of α1-adrenoceptor in brain. Front Mol Biosci. 2020;7:586327. [PubMed: 33195432]

22. Xu Y, Wang C, Wey H- Y, et al. Molecular imaging of Alzheimer's disease–related gamma-secretase in mice and nonhuman primates. J Exp Med. 2020;217(12):20182266.

23. Jiang Y, He L, Green J, et al. Discovery of second-generation NLRP3 inflammasome inhibitors: design, synthesis, and biological characterization. J Med Chem. 2019;62(21):9718–9731. [PubMed: 31626545]

24. Liu P, Hamill TG, Chioda M, et al. Discovery of MK-3168: a PET tracer for imaging brain fatty acid amide hydrolase. ACS Med Chem Lett. 2013;4(6):509–513. [PubMed: 24900701]
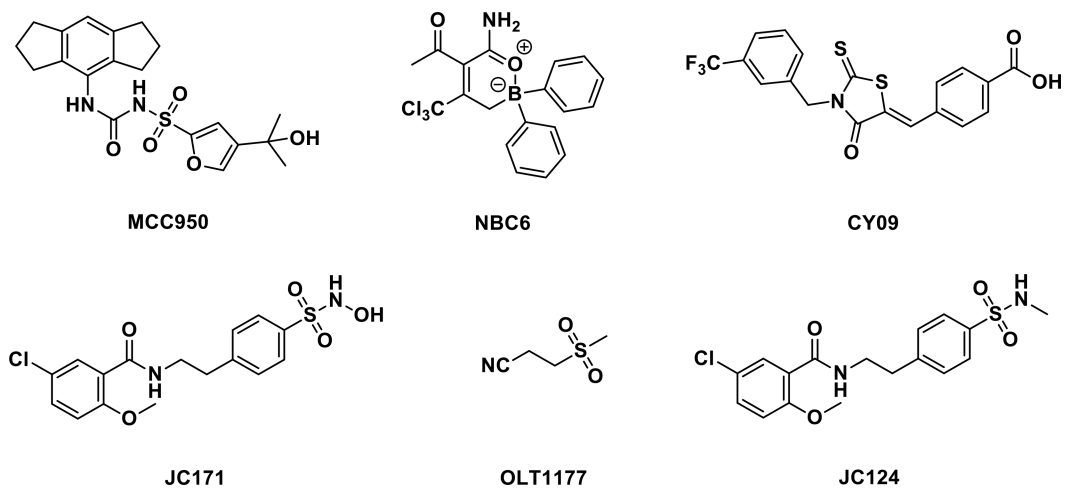
Fig. 1.
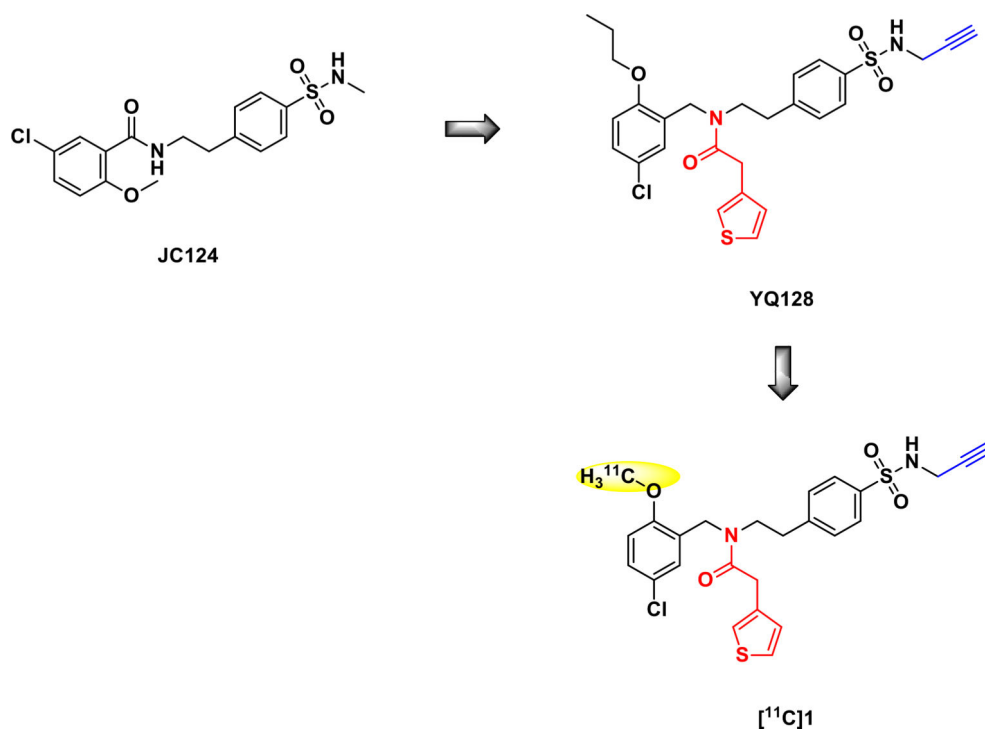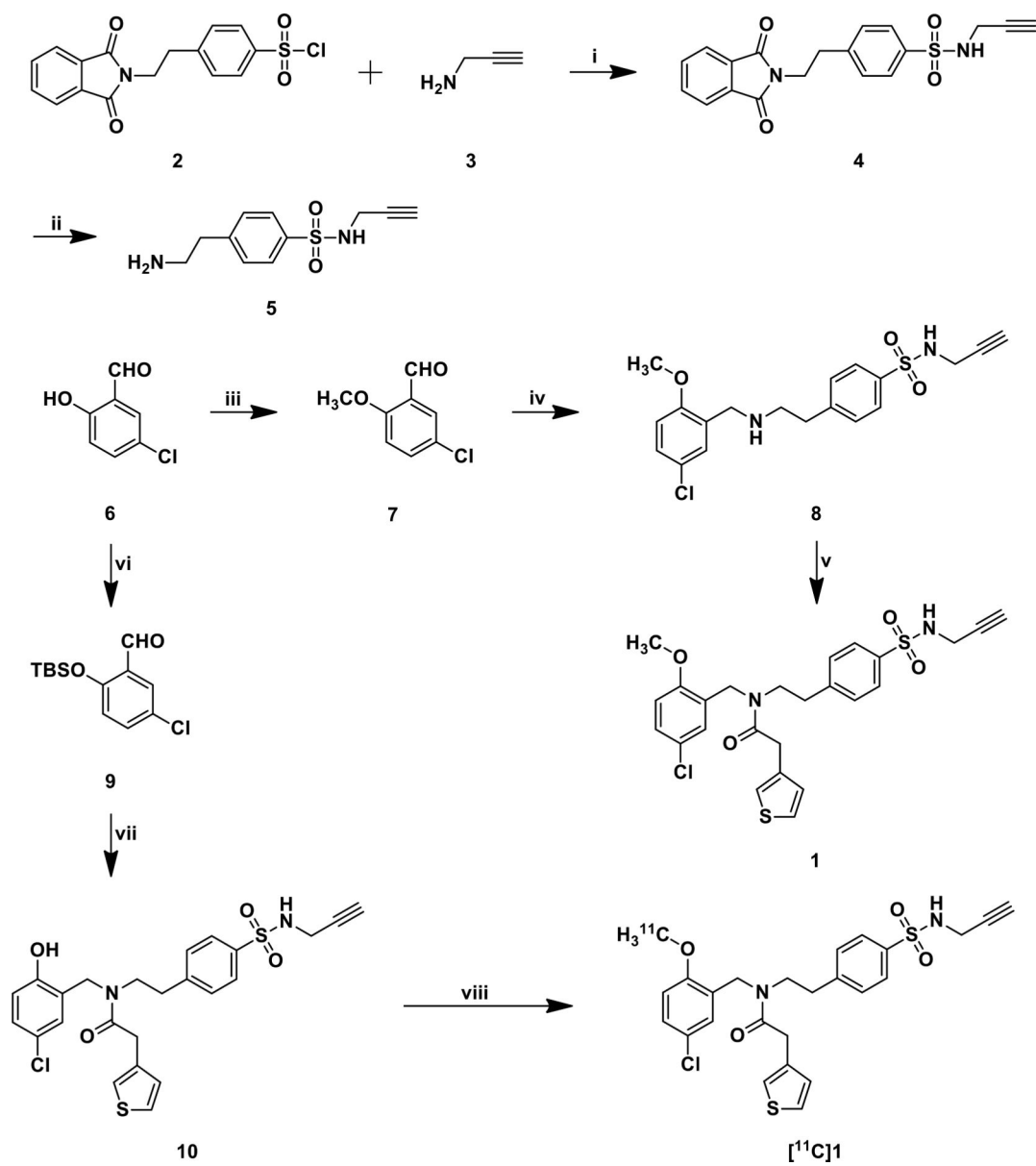Structures of some representative NLRP3 inflammasome inhibitors.

Fig. 2.
Design of the NLRP3 PET tracer in our group.

Scheme 1.
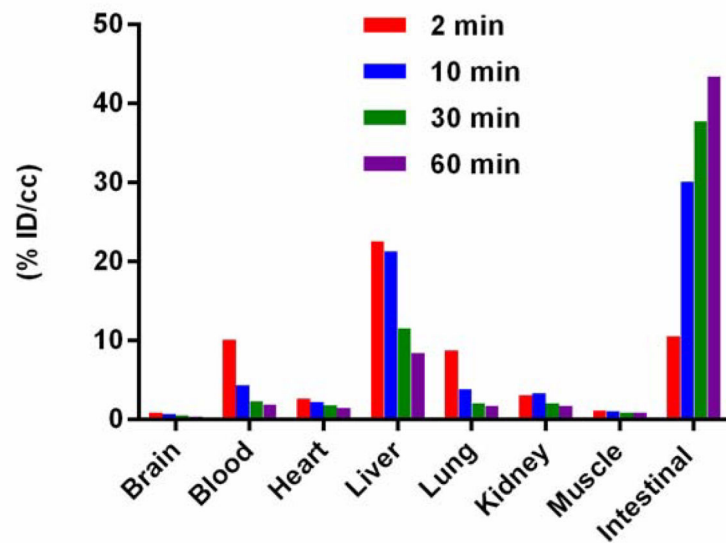Synthesis of sulfonamide derivative **1** and [**^{11}C**]**1**[a]

Fig. 3.
Biodistribution histogram of **[^{11}C]1** in C57BL/6 mice. All data are the mean. Data are expressed as the percentage of injected dose per cubic centimeter (% ID/cc).
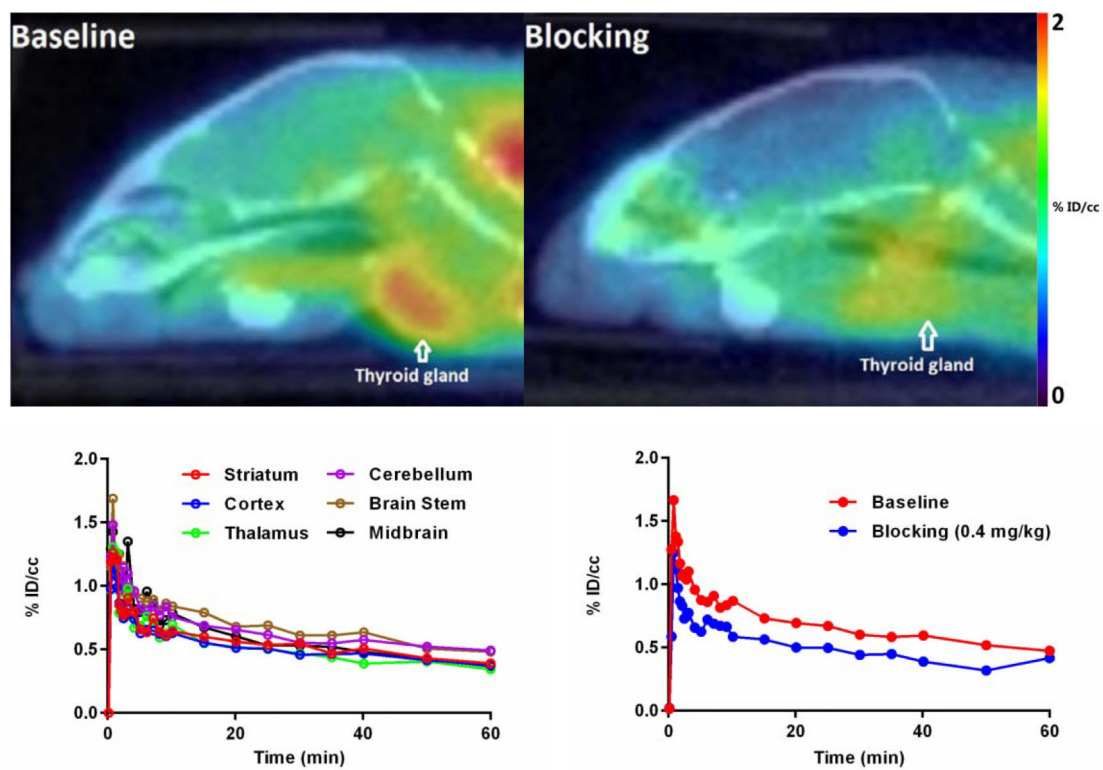
Fig. 4.
Above: Sagittal PET/CT images of [^{11}C]1 in baseline and blocking experiments (summed 15–60 mins). Below (left): Baseline TACs in six representative mouse brain regions. Below (right): TACs of baseline and blocking experiments in C57BL/6 mouse brains. All data are the mean. Data are expressed as the percentage of injected dose per cubic centimetre (% ID/cc).